

O.Z.I. Abu Ibaid, S. Belhamdi, M. Abid, S. Chakroune, S. Mouassa, Z.S. Al-Sagar

Wavelet packet analysis for rotor bar breakage in an inverter induction motor

Introduction. In various industrial processes, squirrel cage induction motors are widely employed. These motors can be used in harsh situations, such as non-ventilated spaces, due to their high strength and longevity. These machines are subject to malfunctions such as short circuits and broken bars. Indeed, for the diagnosis several techniques are offered and used. **Novelty** of the proposed work provides the use of wavelet analysis technology in a continuous and discrete system to detect faults affecting the rotating part of an induction motor fed by a three-phase inverter. **Purpose.** This paper aims to present a novel technique for diagnosing broken rotor bars in the low-load, stationary induction machine proposed. The technique is used to address the problem of using the traditional Techniques like Fourier Transforms signal processing algorithm by analyzing the stator current envelope. The suggested method is based on the use of discrete wavelet transform and continuous wavelet transform. **Methods.** A waveform can be monitored at any frequency of interest using the suggested discrete wavelet transform and continuous wavelet transform. To identify the rotor broken bar fault, stator current frequency spectrum is analyzed and then examined. Based on a suitable index, the algorithm separates the healthy motor from the defective one, with 1, 2 and 3 broken bars at no-load. **Results.** In comparison to the healthy conditions, the recommended index significantly raises under the broken bars conditions. It can identify the problematic conditions with clarity. The possibility of detecting potential faults has been demonstrated (broken bars), using discrete wavelet transform and continuous wavelet transform. The diagnostic method is adaptable to temporary situations brought on by alterations in load and speed. Performance and efficacy of the suggested diagnostic method are demonstrated through simulation in Simulink® MATLAB environment. References 31, figures 11.

Key words: squirrel cage induction motors, rotor broken bar, continuous wavelet transform, discrete wavelet transform.

Вступ. У різних промислових процесах широко використовуються асинхронні двигуни із короткозамкненим ротором. Ці двигуни можуть використовуватися в суворих умовах, наприклад, в приміщеннях, що не вентилюються, завдяки їх високій міцності і довговічності. Ці машини схильні до несправностей, таких як коротке замикання і зламані стрижні. Зрозуміло, що для діагностики пропонується та використовується кілька методик. **Новизна** запропонованої роботи полягає у використанні технології вейвлет-аналізу в безперервній і дискретній системі для виявлення несправностей, що впливають на частину асинхронного двигуна, що обертається, що живиться від трифазного інвертора. **Мета.** У цій статті представлена нова методика діагностики зламаних стрижнів ротора в малонавантаженої стаціонарній асинхронній машині. Цей метод використовується для вирішення проблеми використання традиційних методів, таких як алгоритм обробки сигналів перетворення Фур'є, шляхом аналізу огибаючої струму статора. Пропонуваний метод заснований на використанні дискретного вейвлет-перетворення та безперервного вейвлет-перетворення. **Методи.** Форма сигналу може відстежуватися на будь-якій частоті, що цікавить, з використанням запропонованого дискретного вейвлет-перетворення і безперервного вейвлет-перетворення. Для виявлення несправності обриву стрижня ротора частотний спектр статора аналізується, а потім досліджується. На основі відповідного індексу алгоритм відокремлює справний двигун від несправного з 1, 2 і 3 зламаними стрижнями на холостому ході. **Результати.** Порівняно із нормальними умовами рекомендований показник значно підвищується за умов зламаних стрижнів. Він може чітко визначити проблемні умови. Було продемонстровано можливість виявлення потенційних несправностей (зламани стрижні) з використанням дискретного вейвлет-перетворення та безперервного вейвлет-перетворення. Метод діагностики адаптується до тимчасових ситуацій, викликаних змінами навантаження та швидкості. Працездатність та ефективність запропонованого методу діагностики продемонстровано за допомогою моделювання у середовищі Simulink® MATLAB. Бібл. 31, рис. 11.

Ключові слова: асинхронні двигуни з короткозамкненим ротором, зламаний стрижень ротора, безперервне вейвлет-перетворення, дискретне вейвлет-перетворення.

Introduction. Currently, induction motors are very popular in the industry and is of great interest to scientists in the variable speed drive. Since of their robust construction, high power-to-weight ratio, high reliability and easy design, squirrel cage induction motors are used in most industries [1]. They are, however, susceptible to failures, which may be caused by the machine itself or by operating conditions.

They found flaws in the converter and inverter of an induction motor that was functioning. In order to apply variable speed applications to the induction motor, an inverter is necessary [2].

According to failure studies, induction motor component failure is typical:

- Stator related (38 %);
- Rotor related (10 %);
- Bearing related (40 %); and others (12 %) [3].

The induction motor could be saved from catastrophic harm if the defect is detected quickly.

Even early detection of an issue could cut down on the amount of time necessary for maintenance. The most prevalent rotor defects are located at the level of the rotor, where bar breakage is the most common rotor problem. It

might be at the notch or at the end of the rotor ring that connects it to the rotor ring [4].

Damage to the machine may result from the fractured rotor bar's fault, which increases fluctuation and reduces the amplitude of the torque. As a result, additional mechanical vibrations and fluctuation may be produced. Ultimately, the increased number of damaged bars makes their effect more obvious [5]. To avoid such issues, the technique of fault diagnosis and identification has become a crucial step in protecting this sort of electrical machines. The sorts of faults often relate to diagnostic techniques [6-9].

In recent years, many researchers have been drawn to motor current signature analysis because of its benefits. Current spectral analysis as it has been done in [10].

The benefit of signal processing techniques such as Fourier Fast Transformation (FFT) Wavelet theory is that it provides a coherent framework for a variety of approaches developed for distinct signal processing applications [11, 12].

Over the past 15 years, there has been a significant amount of research on the development of different steady-state condition monitoring approaches, most of which are based on the FFT.

This theory is distinguished from others in that it is faster in signal analysis, which provides ease in dealing and saves time. Therefore, it was briefly discussed due to its value in scientific research and the renaissance of industrial maintenance [13].

The wavelet transform (WT) is a signal analysis method for time-varying or non-stationary signals that uses a description of spectral decomposition using the scaling idea for fault detection. This approach works well for both stationary and non-stationary signal processing [14].

In order to improve the broken rotor bar diagnosis in induction motors under low load, the researcher developed [15], which combines the Hilbert transform with the neural network operation. The stator current envelope is extracted using the Hilbert transform. After then, FFT is used to process this signal. The fault frequency must be extracted. Under various stress circumstances, this approach is used to count the number of broken rotor bars.

The study of flaws in another approach is employed for broken rotor bars detection in [16] utilizing a lower sampling rate and fewer samples. To address this issue, a novel method based on the pitch synchronous WT at a reduced sample rate is used.

While [17] took a different approach, he did think about diagnostic strategies utilizing electrical signal spectral analysis. These techniques can be classified into two categories: internal diagnosis using a model of the motor based on its parameters, and external diagnosis utilizing external signals, which does not require knowledge of motor properties.

Additionally, [18] had advanced a broken rotor bar fault detection using the power of the sidebands in his investigation of flaws. When the motor is linked directly to the supply voltage, this method is applied to the line current and instantaneous power of one stator phase.

The degree of the defect (such as partial or multiple broken rotor bars), motor loading, the impacts of the starting rotor position, supply imbalance, and the variations in the 3 phase currents are not examined in these early research. Furthermore, the addition of an inverter to an induction motor represents a variety of technology that was not examined in the investigations. We were obviously focused on how crucial the inverter was for using the induction motor with variable speed applications.

The goal of the paper is to use Wavelet Packet Transform on current window frame samples from an induction motor to diagnose and categorize broken rotor bars using Discrete Wavelet Transforms (DWT) and Continuous Wavelet Transform (CWT).

Basic calculation relationships and assumptions.

Figure 1 shows the diagram of the impeller failure circuit of the induction machine, with equivalent resistance, in the case of broken bars [19].

According to the reference frame (d-q) fixed to the rotor [19, 20], the model for a three-phase induction motor is:

$$[V] = [R] \cdot [I] + \frac{d}{dt} [[L] \cdot [I]], \quad (1)$$

where:

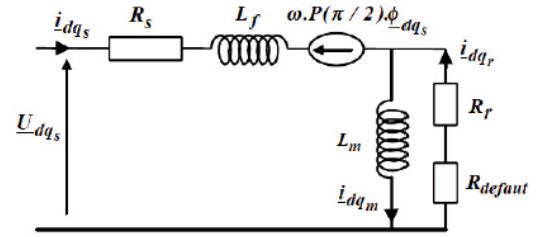


Fig. 1. Broken rotor bars mode

$$\begin{bmatrix} L_{sc}I_2 & -\frac{N_r}{2}M_{sr}I_2 & \vdots & 2 \\ -\frac{3}{2}M_{sr}I_2 & I_{rdq} & \vdots & 0 \\ \dots & \dots & \dots & \dots \\ 0 & 0 & 0 & L_e \end{bmatrix} \frac{d}{dt} \begin{bmatrix} i_{dqs} \\ i_{dqr} \\ \dots \\ i_e \end{bmatrix} = \begin{bmatrix} V_{dqs} \\ V_{dqr} \\ \dots \\ V_e \end{bmatrix} \quad (1)$$

$$\begin{bmatrix} R_s I_2 + \omega_r L_{sc} J_2 & -\frac{N_r}{2} \omega_r M_{sr} J_2 & \vdots & 0 \\ 0 & R_{rdq} J_2 & \vdots & 0 \\ \dots & \dots & \dots & \dots \\ 0 & 0 & \vdots & R_e \end{bmatrix} \begin{bmatrix} i_{dqs} \\ i_{dqr} \\ \dots \\ i_e \end{bmatrix}; \quad (2)$$

$$L_{rdq} = L_{rp} - M_{rr} + \frac{2L_e}{N_r} + 2L_e(1 - \cos(a)); \quad (2)$$

$$R_{rdq} = 2 \cdot \frac{R_e}{N_r} + 2R_b(1 - \cos(a)); \quad (3)$$

$$I_2 = \begin{bmatrix} 1 & 0 \\ 0 & 1 \end{bmatrix}; \quad J_2 = \begin{bmatrix} 0 & -1 \\ 1 & 0 \end{bmatrix}; \quad [R_{rdq}] = \begin{bmatrix} R_{rdd} & R_{rdq} \\ R_{rqd} & R_{rqq} \end{bmatrix},$$

where the 4 terms of this matrix are:

$$R_{rdd} = 2R_b \cdot (1 - \cos(a)) + 2 \cdot \frac{R_e}{N_r} + \frac{2}{N_r} \cdot (1 - \cos(a)) \times \sum_k R_{bfk} (1 - \cos(2k-1)a);$$

$$R_{rqq} = 2R_b \cdot (1 - \cos(a)) + 2 \cdot \frac{R_e}{N_r} + \frac{2}{N_r} \cdot (1 - \cos(a)) \times \sum_k R_{bfk} (1 + \cos(2k-1)a);$$

$$R_{rdq} = -\frac{2}{N_r} \cdot (1 - \cos(a)) \sum_k R_{bfk} \cdot \sin(2k-1)a;$$

$$R_{rqd} = -\frac{2}{N_r} \cdot (1 - \cos(a)) \sum_k R_{bfk} \cdot \sin(2k-1)a.$$

Electromagnetic couples are expressed as:

$$C_e = \frac{3}{2} \cdot p \cdot N_r \cdot M_{sr} \cdot (I_{ds} \cdot I_{qr} - I_{qs} \cdot I_{dr}). \quad (4)$$

Signal processing methods. In order to detect problems and overloads in electric devices, especially those used to generate energy and drive high-capacity motors. Advances in microelectronics and signal processing are accelerating the development of contemporary diagnostic technologies [21]. Because temporal patterns don't convey much information, we must rely on signal processing techniques [22]. Spectral analysis has long been used to detect faults in electrical machines, such as asynchronous machine rotor bar breakage, bearing degeneration, eccentricity, and winding short circuits. We'll go over some cutting-edge techniques like FFT and WT briefly in [23].

Wavelet Transform is a sophisticated approach for improving stator current data analysis in the transform.

Continuous Wavelet Transform. It's common to want to distinguish between lower frequencies bands than DWT permits.

Using the CWT, this is conceivable [24]. The signal's CWT is expressed as follows:

$$CWT(a,b) = \frac{1}{\sqrt{a}} \int_{-\infty}^{+\infty} x(t) \varphi^* \left(\frac{t-b}{a} \right) dt, \quad (5)$$

where $\varphi(t)$ is the mother wavelet, which represents a disputed function in the time and frequency domains; $\varphi^*(t)$ is the mother wavelet's complex conjugates, an is the scale value; b is the translation value. In a more compact form, the normalized wavelet function is:

$$\varphi(a,b) = \frac{1}{\sqrt{a}} \varphi^* \left(\frac{t-b}{a} \right). \quad (6)$$

The integral equation is rewritten as:

$$CWT(a,b) = \int_{-\infty}^{+\infty} x(t) \varphi_{a,b}^*(t) dt. \quad (7)$$

Discrete Wavelet Transforms. The wavelet analysis (WT) is a sophisticated approach for improving stator current data analysis in the transitional or stable states [25].

Because of the DWT's automatic filtering, the tool offers a lot of flexibility for analyzing the transient evolution of several different frequency components in the same signal at the same time. The computational needs are low as compared to other tools. Furthermore, the DWT is included in most commercial software packages. As a result, no complex or specific algorithm is necessary [3].

Without data loss or redundancy, this technique provides an approximation coefficient containing low frequencies information and a detail coefficient carrying high frequencies information of the original signal at each level [26].

In other words, a signal's Fourier analysis is the sum of several sinusoidal functions, but a signal's WT is the sum of multiple functions that are displaced and scaled replicas of the main function [27]. The technique can be repeated on multiple levels, resulting in the tree structure depicted in Fig. 2 [10].

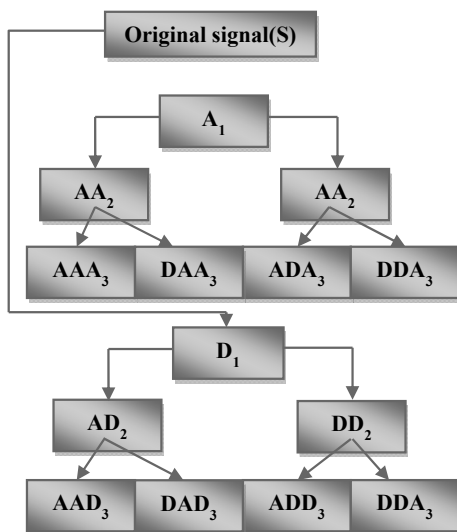


Fig. 2. Decomposition of the signal S in wavelet packet

DWT decomposes a sampled signal $S = (S_1, S_2, \dots, S_n)$ into numerous wavelet signals an approximation signal a_n , and n detail signals d_j ($j \in [1, n]$) [16].

Each frequency band's energy eigenvalue is defined as:

$$E_j = \sum_{k=1}^{k=n} [D_{j,k}(n)]^2; \quad (8)$$

where $j = 1, 2, 2^{n+1}$; n denotes the discrete wavelet decomposition time; D_i denotes the amplitude of the wavelet coefficient of the signal in the associated frequency band in each discrete point as shown in Fig. 3 [28].

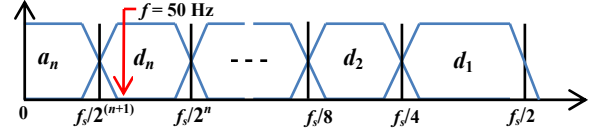


Fig. 3. Filtering process performed by the DWT

FFT is a prominent approach for fault identification in asynchronous devices. It excels in applications requiring great power or steady torque.

The FFT analysis of the bearing fault component will reveal all of the fault's features, including frequency and magnitude responses.

Its purpose is to show how harmonic amplitude grows over time, which is a sign that validates a number of crucial truths [29].

FFT is a technique for decomposing a set of detailed signal spectrum values from one domain to another. Each stage of the procedure consists of a signal spectrum that may be processed with a limited quantity of data to determine the dataset's variation [2 – 22].

The FFT technique can detect flaws in induction motors using this fluctuation. As a result, in signal analysis, the procedure will be faster than DWT [30].

The FFT data can be analyzed as [31]:

$$x(t) = \int_{-\infty}^{+\infty} x(t) \cdot e^{-j \cdot 2 \cdot \pi \cdot f \cdot t} dt. \quad (9)$$

The assessment of a signal is a known interval, which necessitates the selection of a weighting window (Blackmann window, Hanning window, Hamming window, etc.) as well as the window size, which influences the resolution. The frequency accuracy is, in fact, proportional to the sampling frequency and the number of samples N :

$$\Delta f = f_s / N. \quad (10)$$

Simulation results and discussion. We can study the evolution of time elements such as stator currents, torque and speed when the rotor cage shows no failure; starting takes place off-load at nominal voltage with a power supply provided by a three-phase inverter as shown in Fig. 4. The simulation is run over a period of 5 s, with a broken bar occurring at the moment $t = 2$ s and the machine being exposed to a load torque of 3.5 N·m at the instant $t = 0.6$ s. Figure 5 presents the simulation results of the model induction motor, squirrel cage induction machine parameters are shown in Table 1.

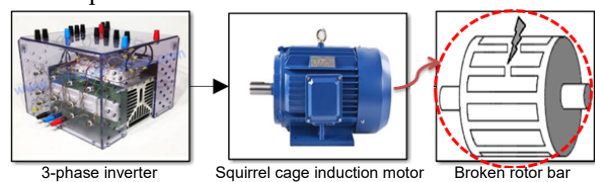


Fig. 4. Simulink block of the induction motor with rotor fault

Table 1

Squirrel cage induction machine parameters	
Parameter	Value
Stator resistance R_s, Ω	7.58
Rotor resistance R_r, Ω	6.3
Number of turns per stator phase, N_s	160
Inertia $J, \text{kg}\cdot\text{m}^2$	0.0054
Resistance of a rotor bar $R_b, \text{m}\Omega$	0.15
Leakage inductance of end ring $L_e, \mu\text{H}$	0.1
Length of the rotor L, mm	65
Mutual inductance L_{1s}, H	0.0265
Stator frequency, Hz	50
Number of rotor bars N_r	16
Poles number p	2
Resistance of end ring segment $R_e, \text{m}\Omega$	0.15
Rotor bar inductance $L_b, \mu\text{H}$	0.1
Air-gap mean diameter E, mm	25
Output power P, kW	1.1

The induction motor was tested under loading conditions first with a healthy rotor, then with 2 broken rotor bars. Every stator current displayed in the study is given in the frequency domain.

The evolution of phase a stator current, electromagnetic torque and phase A current spectrum are illustrated in Fig. 5–7.

We observe from Fig. 5 that the constant current, the electromagnetic torque and the rotational speed that their evolution is constant and also in an excellent and stable condition, so that the speed of the curve increases to reach the ceiling of its peak to settle as a smooth stable plateau.

We notice when 2 adjacent rods are broken, as we note in Fig. 6 in our work, that the speed of rotation decreases gradually, while the ripples also increase more for the constant current in its cover is proportional to the number of broken rods. In a direct relationship, the electromagnetic torque increases with the ripples.

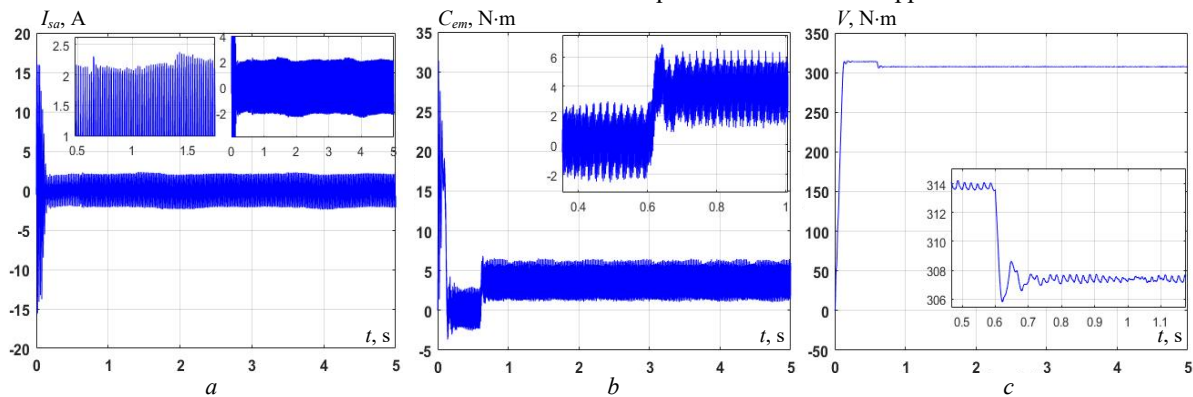


Fig. 5. *a* – evolution of phase A stator current at no-load, on load (healthy); *b* – evolution of the electromagnetic torque on starting, under load (healthy); *c* – rotational speed at start, under load (healthy)

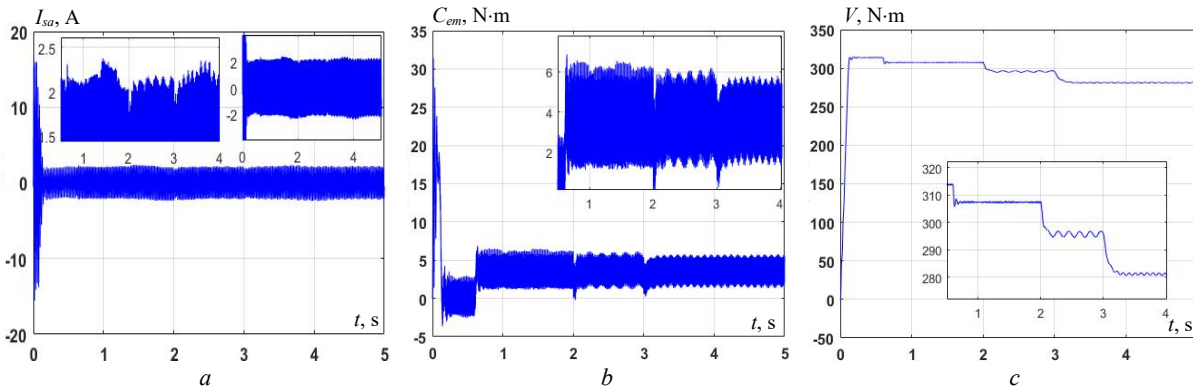


Fig. 6. *a* – evolution of phase A stator current at no-load, on load, then during bar breakage; *b* – evolution of the electromagnetic torque at start-up, under load, then during bar breakage; *c* – rotation speed at start-up, under load, then when the 2 bar breaks

The simulation of the model allowed us to obtain the different characteristics of stator current, speed and electromagnetic torque.

We notice here from Fig. 7,*a* that the spectral stator current in the healthy state does not register any side line around the base line at 50 Hz. As in Fig. 7,*b*, when the machine is loaded, the speed reaches the nominal value and then decreases slightly so that the torque tends to the value of the load torque. It also shows us additional side lines around the base line $f_s = 50 \text{ Hz}$ at frequencies $(1 \pm 2 \cdot k \cdot s) \cdot f_s$.

When analyzing the speed ripple effect, other frequency components of stator current due to rotor asymmetry were observed around the fundamental at the following frequencies $f_b = (1 + 2 \cdot k \cdot s) \cdot f_s$.

In the stator current spectrum, more than one higher harmonic component may be induced in the vicinity of the rotor housing harmonics:

$$f_{hk} = Z \left(\frac{N_r}{b} \right) \cdot ((1-s) \pm 1 \pm 2 \cdot k \cdot s). \quad (11)$$

where s is the slip; f_s is the supply frequency; Z is the positive integer; N_r is the number of rotor bars; p is the number of pole pairs; $k = 1, 2, 3 \dots$ and $h = 1, 3, 5 \dots$

Figure 7,*b* displays the harmonic amplitude's increase as proof that a number of essential criteria are met. The emergence of 2 lateral components with frequencies $(1 + 2 \cdot s) \cdot f_s$ and $(1 - 2 \cdot s) \cdot f_s$ to the left and right of the fundamental f_s is caused by the existence of a broken bar fault, and the degree of gravity of the fault line

amplitudes is $(1 + 2 \cdot k \cdot s) \cdot f_s$, suggesting the presence of a two-bar breaking fault.

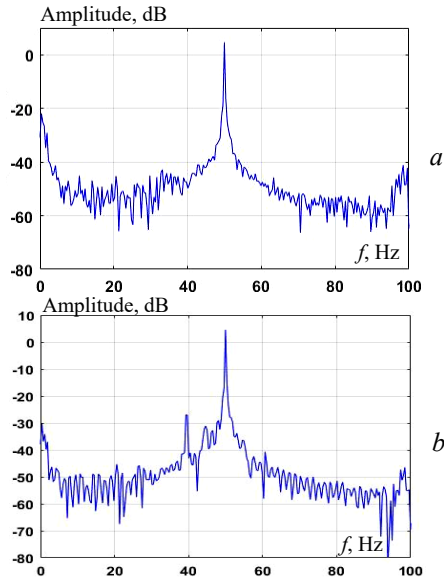


Fig. 7. Phase A current spectrum: a – healthy; b – with bar breaks

Figures 8, 9 demonstrate the use of CWT for stator current for the measurements presented in Fig. 8, 9 for the

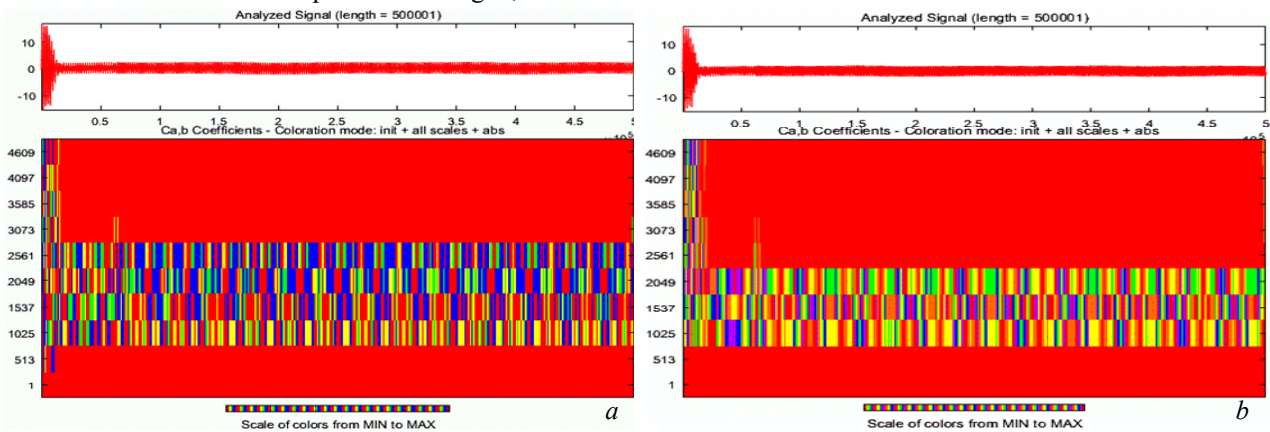


Fig. 8. a – wavelet case of (db); b – wavelet case of (Dmey)

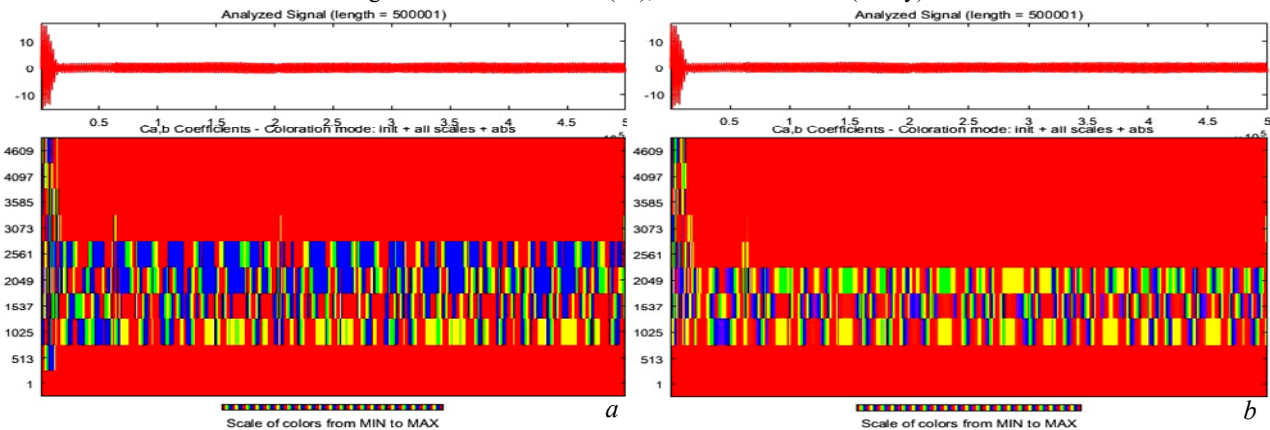


Fig. 9. a – wavelet case of (db) with fault; b – wavelet case of (Dmey) with fault

A closer look at the CWT plots reveals that a healthy motor's starting current displays two patterns under wavelet analysis, the first of which corresponds to the beginning (envelope) and the second of which corresponds to the end (discontinuity) of the signal, while a malfunctioning motor with broken rotor bars displays a third pattern in between the two patterns. It is suggested that this additional pattern can be used to tell a motor that

Meyer family and the family in both a healthy and problematic state of the machine.

Measured using wavelet analysis, the similarity between the signal's fundamental functions (wavelets) and the signal itself is expressed as having the same frequency content. CWT calculated coefficients show how close the signal is to the wave at the current scale.

The current does not alter while the machine is in a healthy state, as opposed to when it is in a damaged one. As the wave coefficients of the kinetic error are stronger than the wave coefficients in the machine's healthy state, we see that the current changes in terms of different degrees of colors and their arrangement in shapes.

These variations show that the wavelet shift may distinguish between the signal components of the healthy and unhealthy motors during the start-up phase. Low frequencies are corresponding to high scales. The higher frequencies match the lower scales.

Another consequence of a broken rotor defect is seen in Fig. 9. The impact is seen in the beginning current envelope plots, where the defective motor starts with a little less current than the healthy motor. This is due to the fact that the defective motor actually has less rotor bars. This is also the cause of the defective motor's decreased torque.

is functioning properly from one that isn't. It is proposed that these variations serve as the distinguishing mark for broken rotor bar fault detection.

Figures 10, 11 show the level signals resulting from the wave decay of the stator current to start in a good health condition of the machine and on the other hand in a defective machine (2 broken bars).

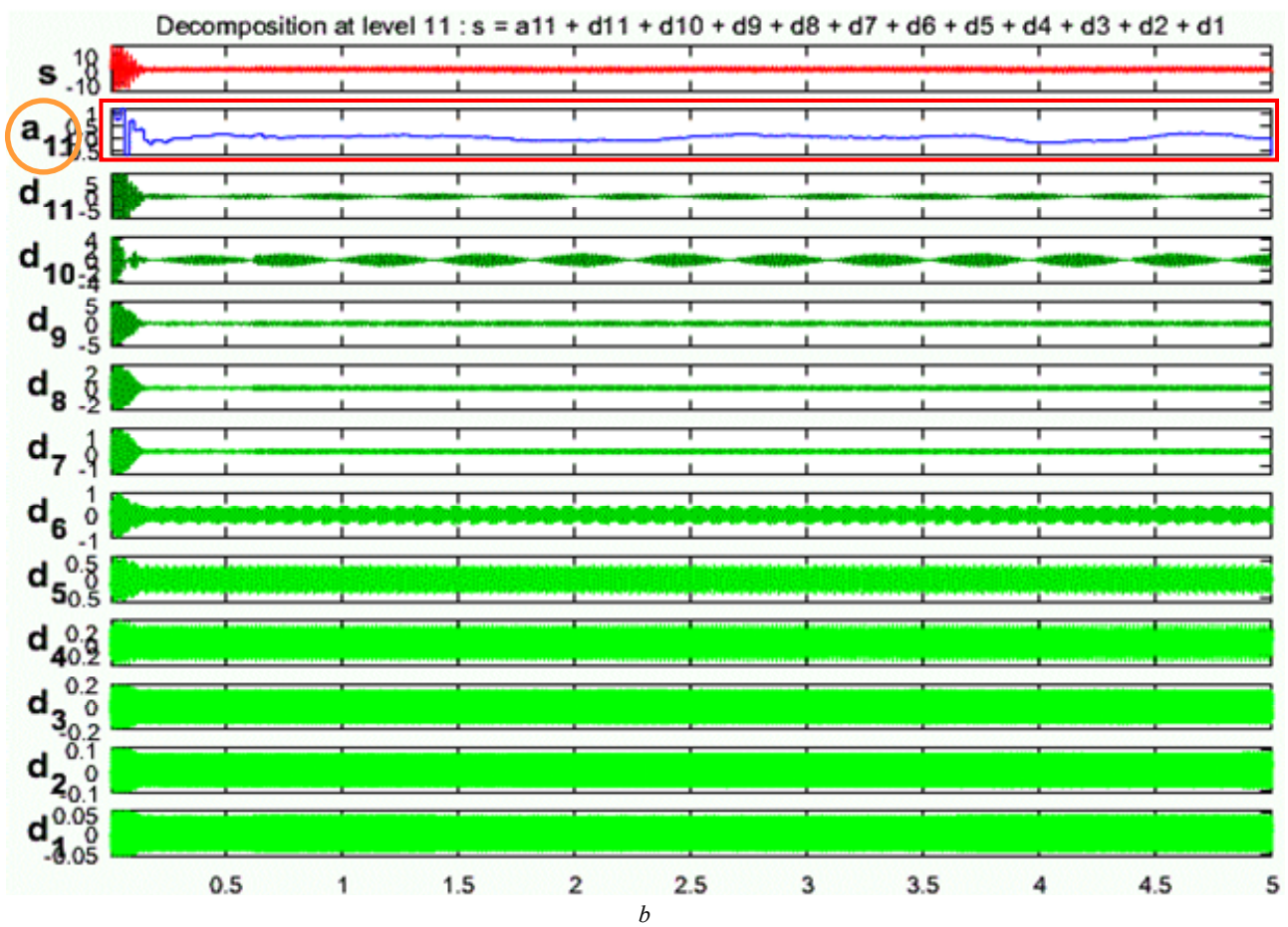
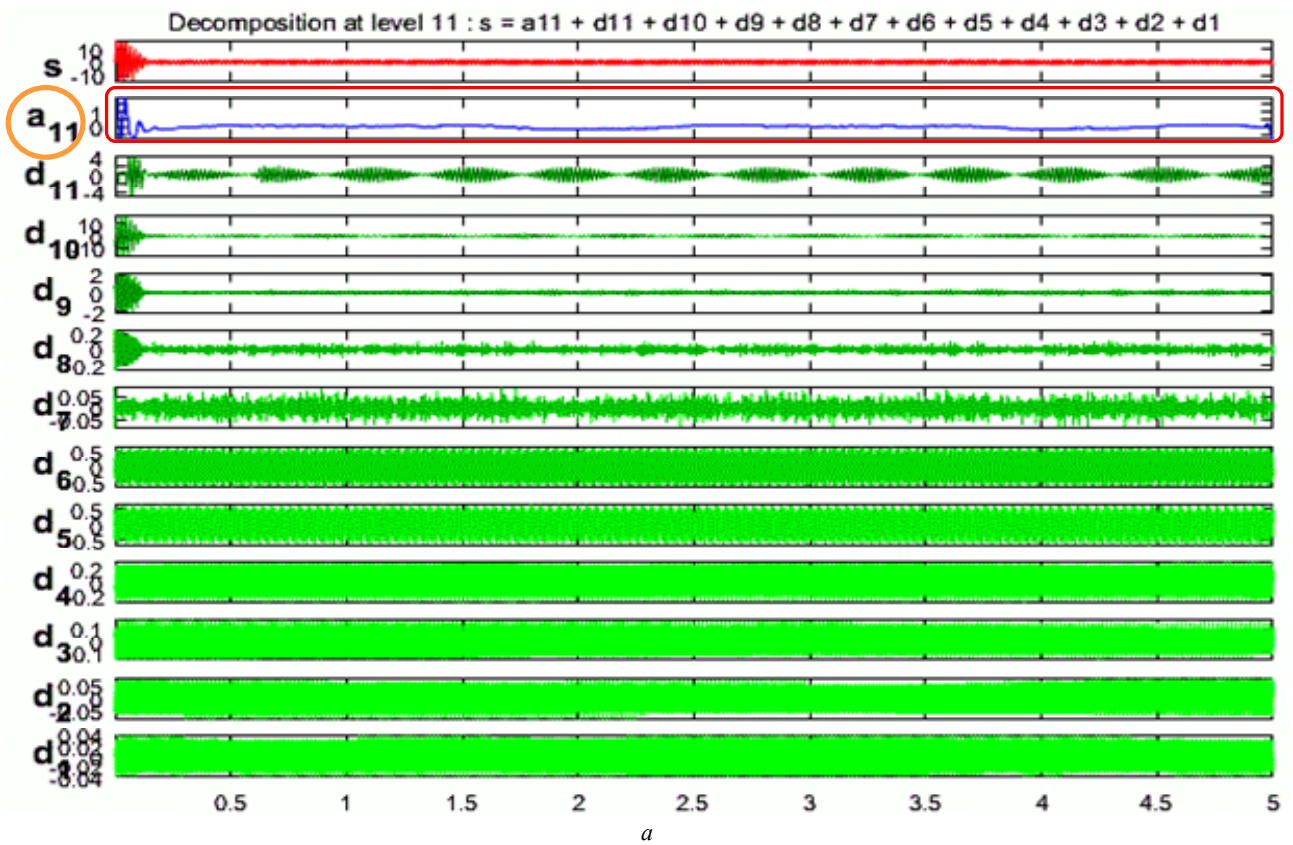


Fig. 10. *a* – wavelet case of sym; *b* – Haar wavelet case

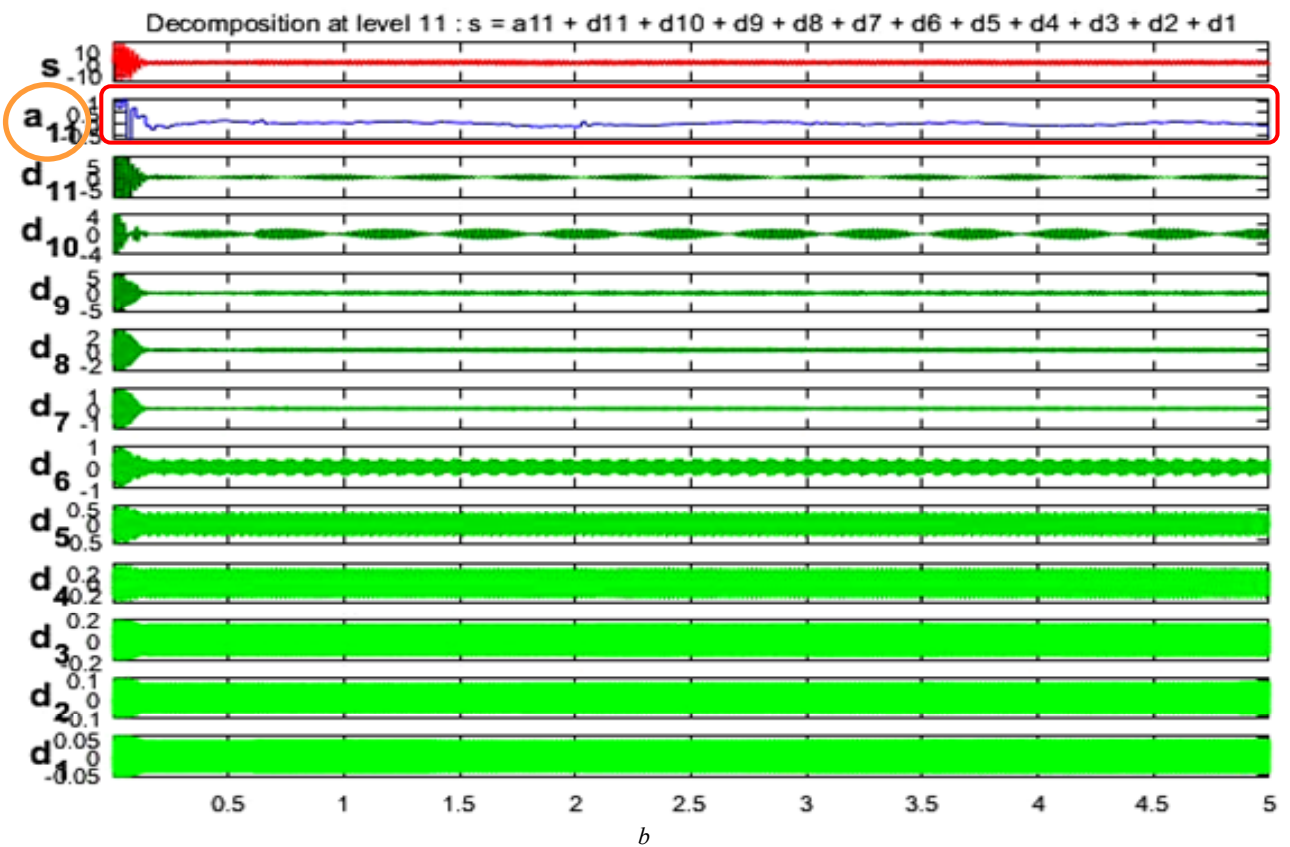
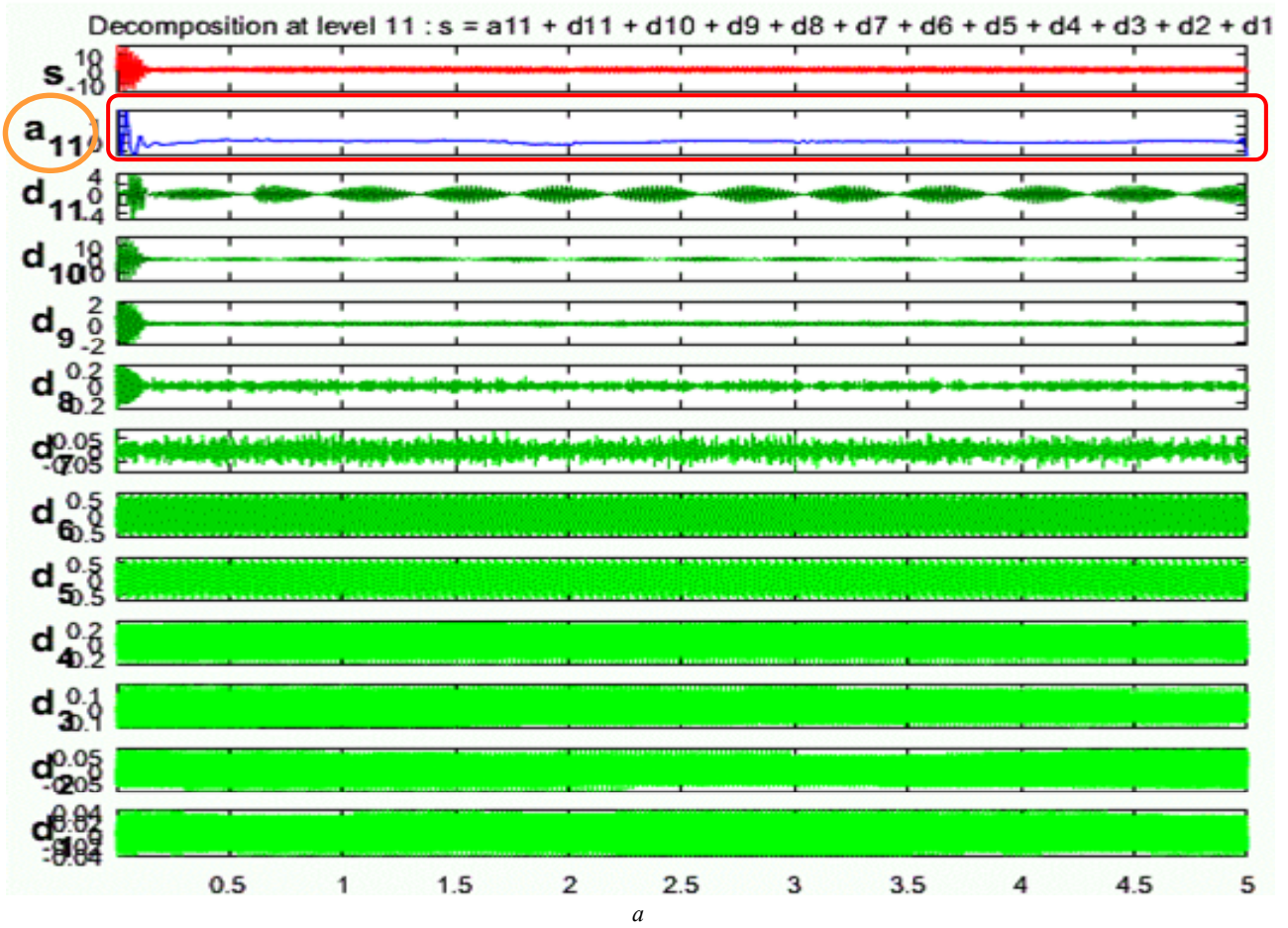


Fig. 11. a – sym wavelet case with fault; b – Haar wavelet case with fault

Gives a precise explanation of the variables brought about by the broken rotor bar fault, describing how harmonics develop under transients and steady-state conditions.

The primary factor in the formation of transitional processes is oscillations. When the wavelet signal strength is high, there is no oscillation in the system. Compared to a healthy state, the stator current magnitude in the faulty condition exhibits high-level coefficients and changes in coefficients.

Failure of broken rotor bars affects the effect of frequency bands, increasing the coefficient. The sampling frequency is set to 5 kHz so that the original signal is decomposed at the 11th level.

The high-frequency information is better explained by the detailed signal, while the low-frequency information is better explained by the approximate signal.

The approximation signal for the 11th level has a frequency range of 2.44 to 1.22 which is a very low frequency so it perfectly diagnoses the faults of the rotor bar.

In general, it is noted that the signal in both cases is not the same and can be identified by the disturbances that appear at high levels.

It is noted that the tenth and 11th levels are better in terms of clarity and useful information than the ninth level, which does not have a significant change.

Through the motor signals and graphs that were taken from the samples and using 11 levels of decomposition, it can be concluded that when the reading started, the motor current showed a greater amplitude due to the higher torque, and then it returns to stability. This information for high and low frequencies about the signal is very useful in providing details. Related to error severity and growth in approximation and detail signals, particularly in the corresponding plane of the frequency band, are validated by evaluating the energy stored in each.

The imbalances produced during the fault appear clearly in the signal « a_{11} ».

Conclusions.

For the purpose of finding faults in squirrel cage induction motors, wavelet packet analysis is an effective tool. The signal is divided into various frequency components using wavelet packets so that any irregularities can be examined. By examining the frequency spectrum of the motor current, the wavelet packet analysis is able to identify broken rotor bar problems. Additionally, it may tell you where the defect is and how serious it is. Wavelet packet analysis can also be used to find other induction motor issues. This makes it a useful tool for identifying and resolving induction motor problems.

In this research, the diagnostic technique is based on the use of discrete wavelet transform and continuous wavelet transform, where it is based on the analysis of the stator current, at the start-up electromagnetic torque.

This method can clearly exhibit the time-frequency characteristic of fault signals. By increasing the peaks of the time domain waveform analysis function, these two techniques' performance was demonstrated by their capacity to produce a local representation of non-stationary current signals for both a functioning machine and one that has a defect.

Conflict of interest. The authors declare no conflict of interest.

REFERENCES

1. Dehina W., Boumehraz M., Kratz F. Diagnosis of Rotor and Stator Faults by Fast Fourier Transform and Discrete Wavelet in Induction Machine. *2018 International Conference on Electrical Sciences and Technologies in Maghreb (CISTEM)*, 2018, pp. 1-6. doi: <https://doi.org/10.1109/CISTEM.2018.8613311>.
2. Rohan A., Kim S.H. Fault Detection and Diagnosis System for a Three-Phase Inverter Using a DWT-Based Artificial Neural Network. *The International Journal of Fuzzy Logic and Intelligent Systems*, 2016, vol. 16, no. 4, pp. 238-245. doi: <https://doi.org/10.5391/IJFIS.2016.16.4.238>.
3. Bessam B., Menacer A., Boumehraz M., Cherif H. DWT and Hilbert Transform for Broken Rotor Bar Fault Diagnosis in Induction Machine at Low Load. *Energy Procedia*, 2015, vol. 74, pp. 1248-1257. doi: <https://doi.org/10.1016/j.egypro.2015.07.769>.
4. Amanuel T., Ghirmay A., Ghebremeskel H., Ghebrehwet R., Bahlibi W. Comparative Analysis of Signal Processing Techniques for Fault Detection in Three Phase Induction Motor. *Journal of Electronics and Informatics*, 2021, vol. 3, no. 1, pp. 61-76. doi: <https://doi.org/10.36548/jei.2021.1.006>.
5. Menacer A., Moreau S., Benakcha A., Said M.S.N. Effect of the Position and the Number of Broken Bars on Asynchronous Motor Stator Current Spectrum. *2006 12th International Power Electronics and Motion Control Conference*, 2006, pp. 973-978. doi: <https://doi.org/10.1109/EPEPEMC.2006.4778526>.
6. Talhaoui H., Ameid T., Kessal A. Energy eigenvalues and neural network analysis for broken bars fault diagnosis in induction machine under variable load: experimental study. *Journal of Ambient Intelligence and Humanized Computing*, 2022, vol. 13, no. 5, pp. 2651-2665. doi: <https://doi.org/10.1007/s12652-021-03172-2>.
7. Ince T. Real-time broken rotor bar fault detection and classification by shallow 1D convolutional neural networks. *Electrical Engineering*, 2019, vol. 101, no. 2, pp. 599-608. doi: <https://doi.org/10.1007/s00202-019-00808-7>.
8. Talhaoui H., Ameid T., Aissa O., Kessal A. Wavelet packet and fuzzy logic theory for automatic fault detection in induction motor. *Soft Computing*, 2022, vol. 26, no. 21, pp. 11935-11949. doi: <https://doi.org/10.1007/s00500-022-07028-5>.
9. Abid M., Laribi S., Larbi M., Allaoui T. Diagnosis and localization of fault for a neutral point clamped inverter in wind energy conversion system using artificial neural network technique. *Electrical Engineering & Electromechanics*, 2022, no. 5, pp. 55-59. doi: <https://doi.org/10.20998/2074-272X.2022.5.09>.
10. Kompella K.C.D., Mannam V.G.R., Rayapudi S.R. DWT based bearing fault detection in induction motor using noise cancellation. *Journal of Electrical Systems and Information Technology*, 2016, vol. 3, no. 3, pp. 411-427. doi: <https://doi.org/10.1016/j.jesit.2016.07.002>.
11. Saidi L., Fnaiech F., Henao H., Capolino G.-A., Cirrincione G. Diagnosis of broken-bars fault in induction machines using higher order spectral analysis. *ISA Transactions*, 2013, vol. 52, no. 1, pp. 140-148. doi: <https://doi.org/10.1016/j.isatra.2012.08.003>.
12. Bouzida A., Touhami O., Abdelli R. Rotor Fault Diagnosis in Three Phase Induction Motors Using the Wavelet Transform. *International Conference on Control, Engineering & Information Technology (CEIT'13). Proceedings Engineering & Technology*, 2013, vol. 1, pp. 186-191. Available at: http://ipco-co.com/PET_Journal/presented%20papers/095.pdf (accessed 24 July 2022).
13. Dehina W., Boumehraz M., Kratz F. Diagnosis and Detection of Rotor Bars Faults in Induction Motor Using HT and DWT Techniques. *2021 18th International Multi-Conference on Systems, Signals & Devices (SSD)*, 2021, pp. 109-115. doi: <https://doi.org/10.1109/SSD52085.2021.9429381>.
14. Hussein A.M., Obed A.A., Zubo R.H.A., Al-Yasir Y.I.A., Saleh A.L., Fadhel H., Sheikh-Akbari A., Mokryani G., Abd-Alhameed R.A. Detection and Diagnosis of Stator and Rotor Electrical Faults for Three-Phase Induction Motor via Wavelet Energy Approach. *Electronics*, 2022, vol. 11, no. 8, art. no. 1253. doi: <https://doi.org/10.3390/electronics11081253>.

15. Cherif H., Menacer A., Bessam B., Kechida R. Stator inter turns fault detection using discrete wavelet transform. *2015 IEEE 10th International Symposium on Diagnostics for Electrical Machines, Power Electronics and Drives (SDEMPED)*, 2015, pp. 138-142. doi: <https://doi.org/10.1109/DEMPED.2015.7303681>.
16. Hassen K., Braham A., Zied L. Diagnosis of broken rotor bar in induction machines using pitch synchronous wavelet transform. *4th International Conference on Power Engineering, Energy and Electrical Drives*, 2013, pp. 896-901. doi: <https://doi.org/10.1109/PowerEng.2013.6635729>.
17. Eltabach M., Charara A., Zein I. A Comparison of External and Internal Methods of Signal Spectral Analysis for Broken Rotor Bars Detection in Induction Motors. *IEEE Transactions on Industrial Electronics*, 2004, vol. 51, no. 1, pp. 107-121. doi: <https://doi.org/10.1109/TIE.2003.822083>.
18. Didier G., Ternisien E., Caspary O., Razik H. Fault detection of broken rotor bars in induction motor using a global fault index. *IEEE Transactions on Industry Applications*, 2006, vol. 42, no. 1, pp. 79-88. doi: <https://doi.org/10.1109/TIA.2005.861368>.
19. Abu Ibaid O.Z.I., Belhamdi S., Abid M., Chakroune S. Diagnosis of rotor faults of asynchronous machine by spectral analysis of stator currents. *5th International Aegean Symposiums on Innovation Technologies & Engineering*, February 25-26, 2022, pp. 102-111. Available at: https://www.aegeanconference.com/files/ugd/614b1f_1930a1802a034e389c403c987ca63644.pdf (accessed 24 July 2022).
20. Choudira I., Khodja D., Chakroune S. Fuzzy Logic Based Broken Bar Fault Diagnosis and Behavior Study of Induction Machine. *Journal Européen Des Systèmes Automatisés*, 2020, vol. 53, no. 2, pp. 233-242. doi: <https://doi.org/10.18280/jesa.530210>.
21. Souad L., Bendiabdallah Youcef M., Samir M., Boukezata. Use of neuro-fuzzy technique in diagnosis of rotor faults of cage induction motor. *2017 5th International Conference on Electrical Engineering - Boumerdes (ICEE-B)*, 2017, pp. 1-4. doi: <https://doi.org/10.1109/ICEE-B.2017.8192148>.
22. Abdelhak G., Sid Ahmed B., Djekidel R. Fault diagnosis of induction motors rotor using current signature with different signal processing techniques. *Diagnostyka*, 2022, vol. 23, no. 2, pp. 1-9. doi: <https://doi.org/10.29354/diag/147462>.
23. Chow T.W.S., Hai S. Induction Machine Fault Diagnostic Analysis With Wavelet Technique. *IEEE Transactions on Industrial Electronics*, 2004, vol. 51, no. 3, pp. 558-565. doi: <https://doi.org/10.1109/TIE.2004.825325>.
24. Mohamed M.A., Hassan M.A.M., Albalawi F., Ghoneim S.S.M., Ali Z.M., Dardeer M. Diagnostic Modelling for Induction Motor Faults via ANFIS Algorithm and DWT-Based Feature Extraction. *Applied Sciences*, 2021, vol. 11, no. 19, art. no. 9115. doi: <https://doi.org/10.3390/app11199115>.
25. Kechida R., Menacer A. DWT wavelet transform for the rotor bars faults detection in induction motor. *2011 2nd International Conference on Electric Power and Energy Conversion Systems (EPECS)*, 2011, pp. 1-5. doi: <https://doi.org/10.1109/EPECS.2011.6126825>.
26. Kompella K.C.D., Mannam V.G.R., Rayapudi S.R. DWT based bearing fault detection in induction motor using noise cancellation. *Journal of Electrical Systems and Information Technology*, 2016, vol. 3, no. 3, pp. 411-427. doi: <https://doi.org/10.1016/j.jesit.2016.07.002>.
27. Behim M., Merabet L., Saad S. Detection and Classification of Induction Motor Faults Using DWPD and Artificial Neural Network: Case of Supply Voltage Unbalance and Broken Rotor Bars. *EasyChair Preprint no. 7756*. Available at: https://easychair.org/publications/preprint_download/TrtH (accessed 24 July 2022).
28. Mehrjou M.R., Mariun N., Karami M., Noor S.B.M., Zolfaghari S., Misron N., Kadir M.Z.A.A., Radzi M.A.M., Marhaban M.H. Wavelet-Based Analysis of MCSA for Fault Detection in Electrical Machine. In *Wavelet Transform and Some of Its Real-World Applications. InTech.*, 2015. doi: <https://doi.org/10.5772/61532>.
29. Cusido J., Romeral L., Ortega J.A., Rosero J.A., Espinosa A.G. Fault Detection in Induction Machines Using Power Spectral Density in Wavelet Decomposition. *IEEE Transactions on Industrial Electronics*, 2008, vol. 55, no. 2, pp. 633-643. doi: <https://doi.org/10.1109/TIE.2007.911960>.
30. Amanuel T., Ghirmay A., Ghebremeskel H., Ghebrehiwet R., Bahlubi W. Comparative Analysis of Signal Processing Techniques for Fault Detection in Three Phase Induction Motor. *Journal of Electronics and Informatics*, 2021, vol. 3, no. 1, pp. 61-76. doi: <https://doi.org/10.36548/jei.2021.1.006>.
31. Martinez-Herrera A.L., Ferrucho-Alvarez E.R., Ledesma-Carrillo L.M., Mata-Chavez R.I., Lopez-Ramirez M., Cabal-Yepez E. Multiple Fault Detection in Induction Motors through Homogeneity and Kurtosis Computation. *Energies*, 2022, vol. 15, no. 4, art. no. 1541. doi: <https://doi.org/10.3390/en15041541>.

Received 24.09.2022

Accepted 23.12.2022

Published 06.05.2023

Ossama Ziad Ibrahim Abu Ibaid¹, PhD,

Saad Belhamdi¹, Professor,

Mimouna Abid², PhD,

Salim Chakroune¹, Professor,

Souhil Mouassa³, Senior Lecturer,

Zuhair S. Al-Sagar⁴, Associate Professor,

¹ Department of Electrical Engineering,

Electrical Engineering Laboratory, University of M'Sila, Algeria,

e-mail: osama.abuibaid@univ-msila.dz;

saad.belhamdi@univ-msila.dz; salim.chakroun@univ-msila.dz

² Department of Electrical Engineering,

L2GEGI Laboratory, University of Tiaret, Algeria,

e-mail: mimouna.abid@univ-tiaret.dz (Corresponding Author)

³ Department of Electrical Engineering,

University of Bouira, Algeria,

e-mail: souhil.mouassa@univ-bouira.dz

⁴ Department of Renewable Energy,

Baqubah Technical Institute, Middle Technical University,

Baghdad, Iraq.

e-mail: Zuhairalsagar@mtu.edu.iq

How to cite this article:

Abu Ibaid O.Z.I., Belhamdi S., Abid M., Chakroune S., Mouassa S., Al-Sagar Z.S. Wavelet packet analysis for rotor bar breakage in an inverter induction motor. *Electrical Engineering & Electromechanics*, 2023, no. 3, pp. 3-11. doi: <https://doi.org/10.20998/2074-272X.2023.3.01>